



Physikalisch-Technische Bundesanstalt  
National Metrology Institute

The following article is hosted by PTB;

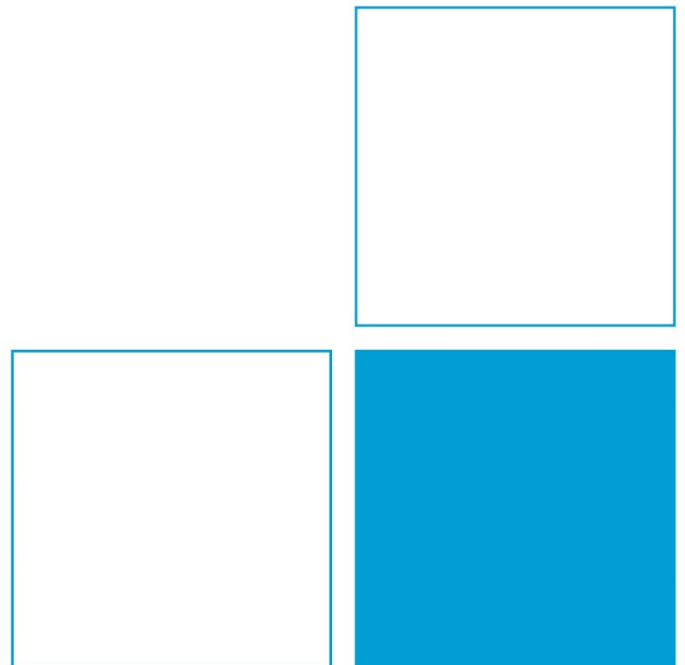
DOI: 10.7795/120.20240627

It is provided for personal use only.

## Round Robin Comparison: MOIF measurements of the stray field distribution of a magnetic scale

**Acknowledgement:** This project (EMPIR 20SIP04 qMOIF) has received funding from the EMPIR programme co-financed by the Participating States and from the European Union's Horizon 2020 research and innovation programme

Available at: <https://doi.org/10.7795/120.20240627>



## Contents

<b>1 Introduction</b> .....	2
<b>2 Sample</b> .....	2
<b>3 Results PTB</b> .....	3
3.1 Calibration of the PTB MagView S.....	3
3.2 Results PTB.....	5
3.3 Comparison PTB data.....	6
<b>4 Results TUBITAK</b> .....	7
4.1 Calibration of the TUBITAK confocal microscope.....	7
4.2 Results TUBITAK.....	8
<b>5 Results Innovent</b> .....	9
5.1 Calibration of the Innovent setup.....	9
5.2 Results Innovent.....	9
<b>6 Comparison between partners</b> .....	10
6.1 PTB and TUBITAK.....	11
6.2 PTB and Innovent.....	11
6.3 Analysis of pole widths.....	12
<b>7 Discussion of uncertainties</b> .....	14

## 1 Introduction

To provide worked examples of quantitative Magneto-Optical Indicator Film measurements in the frame of the EMPIR project 20SIP04qMOIF, Innovent, PTB and TUBITAK performed a Round robin Comparison by measuring the stray field distributions of magnetic scales using the MOIF systems set up in 15SIB06 NanoMag. TUBITAK used its high-resolution microscope. Innovent and PTB used calibrated CMOS-MagView systems. As a secondary parameter, the pole width of the written pole pattern was analyzed.

## 2 Sample

The samples compared in the Round Robin are nominally equal commercial Sensitec scales (tradename: MLI0066HAB-UA) from a sintered hard ferrite material with a written incremental pole pattern with alternating up and down magnetized poles. The poles have a pole width of 1 mm.

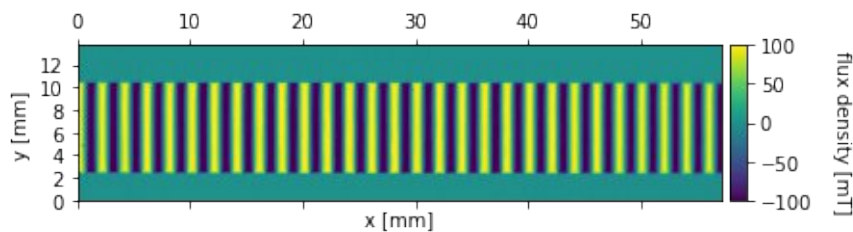


Fig. 1 CMOS-MagView image of a section of the Sensitec scale 3 before it was broken.

One of the scales was broken after the first round of measurements. The now smaller pieces are better suited for measurements on CMOS-MagViews with smaller MOIF. The broken sample is measured with a 500  $\mu\text{m}$  thick PEEK distance plate to reduce the stray field amplitude and thereby to avoid artefacts from high in-plane components.

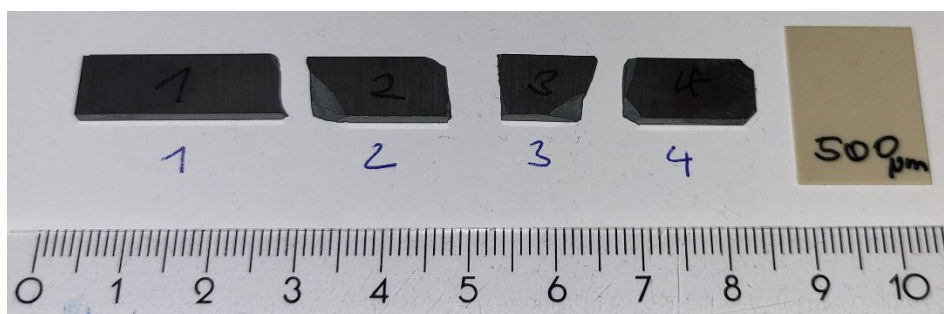


Fig. 2: Photo of the 4 pieces of Scale 3 and of the 500  $\mu\text{m}$  distance plate.

### 3 Results PTB

PTB characterized the scales with 2 Matesy CMOSMagView devices, a CMOS-MagView S and a CMOS-MagView XL with in-plane MOIF and pixel areas of of  $4.5 \mu\text{m} \times 4.5 \mu\text{m}$  and of  $28.4 \mu\text{m} \times 28.4 \mu\text{m}$ , respectively.

#### 3.1 Calibration of the PTB CMOS-MagView S

The PTB CMOS-MagView S was calibrated in an electromagnet with 20 cm pole shoe diameter. A Hall probe was fixed on the MOIF. The external field was varied by applying a current to magnet using a KEPCO BOP 20-20. The room temperature was  $20^\circ\text{C}$ . The CMOS-MagView was switched on and allowed to thermalize for 1 hour. A second set of data was measured 1 hour after finishing the first calibration.

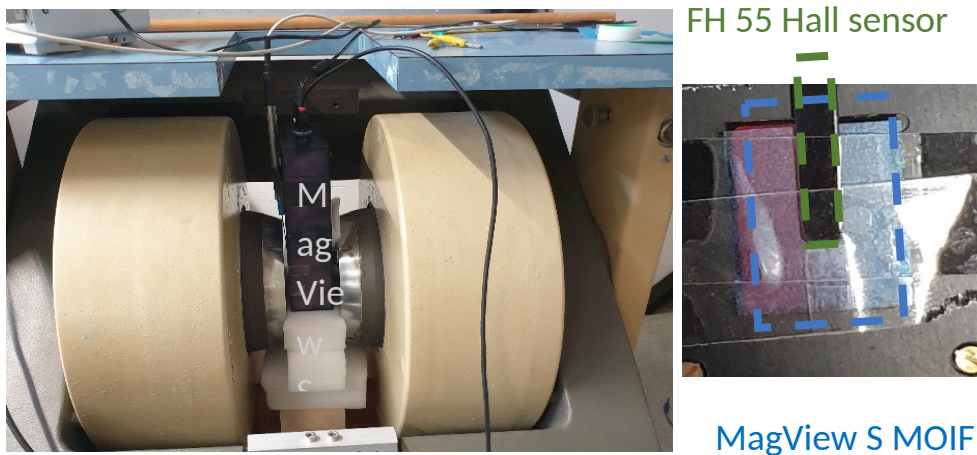


Fig. 3: CMOS-MagView S in the electromagnet used for the calibration (left) and position of the FH55 Hall sensor probe on the MOIF area.

To determine the calibration function, a CMOS-MagView image was taken for each external field value.

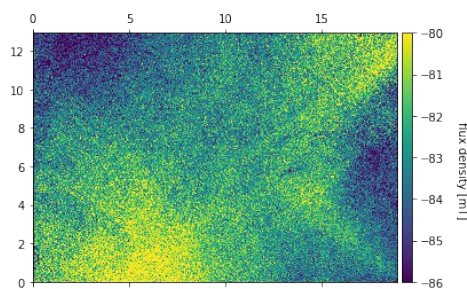


Fig. 4: CMOS-MagView S image taken at an external field of  $-90.1\text{mT}$

The CMOS-MagView measures field amplitude calculated as the average over all pixel values. The thereof resulting standard deviation is used as a measure for the measurement uncertainty.

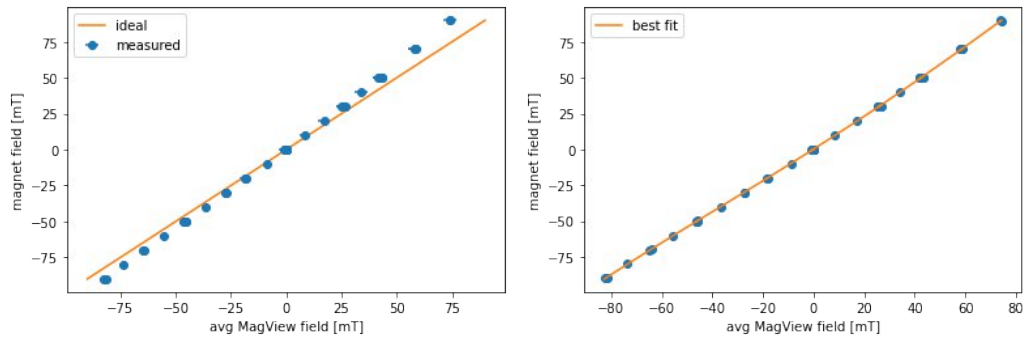


Fig. 5: Results of the calibration and fit function derived from the calibration data

Figure 4 shows the results of the measurement and Figure 5 shows the fitted relation between the averaged CMOS-MagView measured field and the external field. The experimental data are fitted with:

$Y = a + bx + cx^2 + dx^3 + ex^4$ , where

$$a = 0.174 \pm 0.147$$

$$b = 1.124 \pm 0.005$$

$$c = 0.001 \pm 1.47e-04$$

$$d = 5.139e-06 \pm 1.17e-06$$

$$e = -4.340e-08 \pm 2.52e-08$$

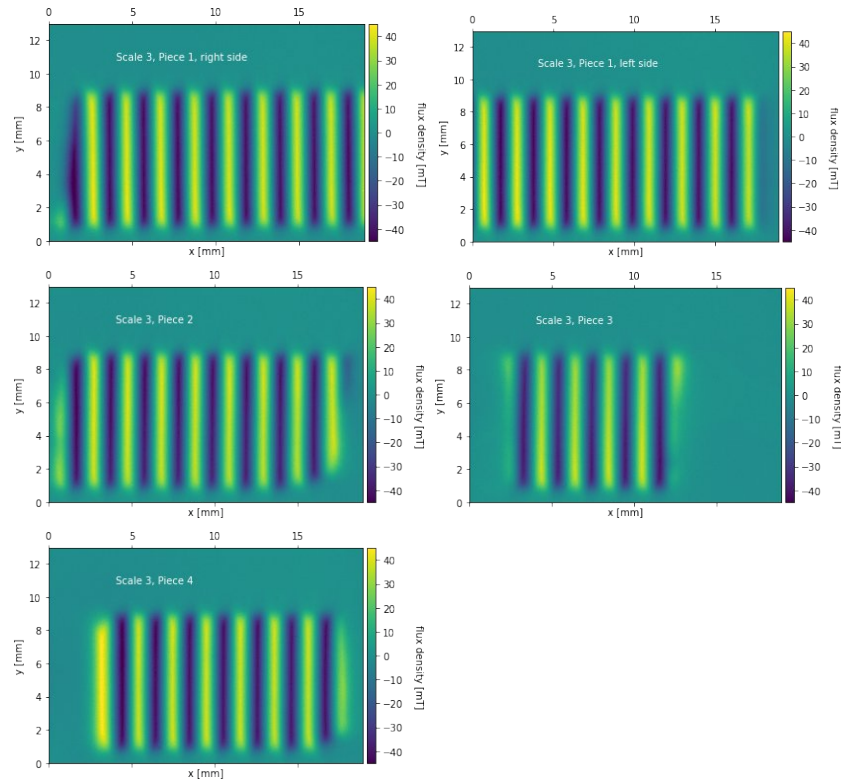
The fit function is used to correct the data of the CMOS-MagView S by calculating a corrected field value for each pixel. The scales were allowed to thermalize by laying them on top of the MagView. This avoids cooling the CMOS-MagView MOIF. Measurements were performed with both PTB MagView devices, the calibrated CMOS-MagView S and with a CMOS-MagView XL which was calibrated before purchasing.

To avoid relevant contributions to the measured signal from high in-plane components of the magnetic flux density a non-magnetic spacer of a thickness of 500  $\mu\text{m}$  (PEEK) was used during the measurements.

### 3.2 Results PTB

PTB data were measured with 2 different CMOS-MagView using a 500  $\mu\text{m}$  thick non-magnetic spacer.

Data CMOS-MagView S:



Data CMOS-MagView XL:

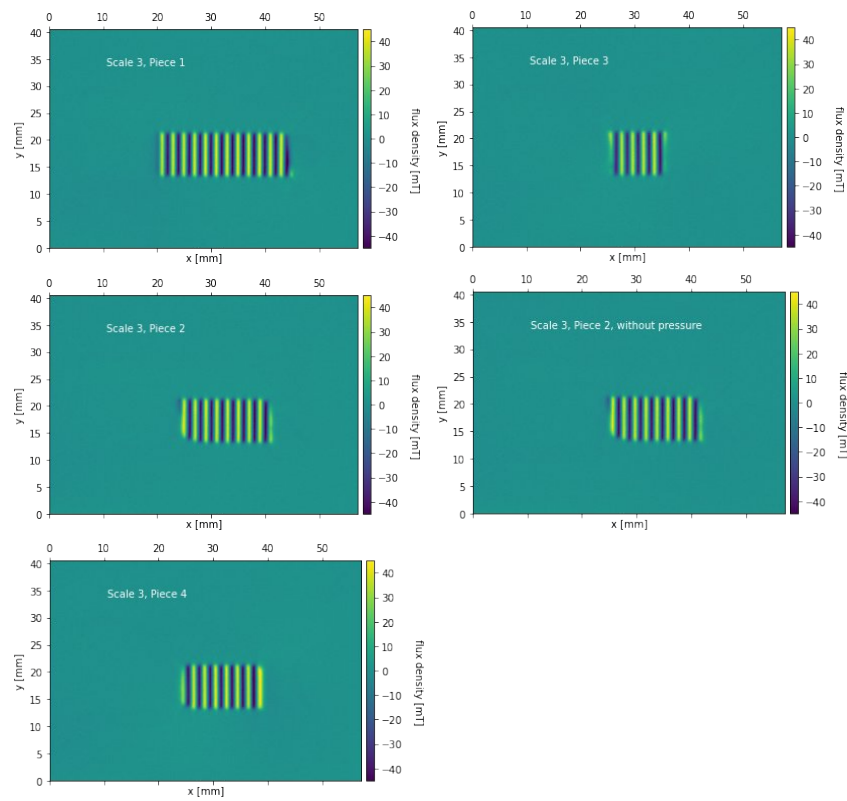
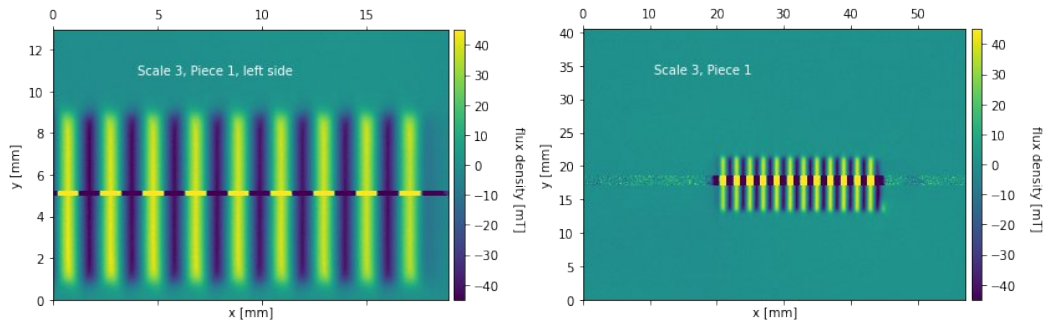


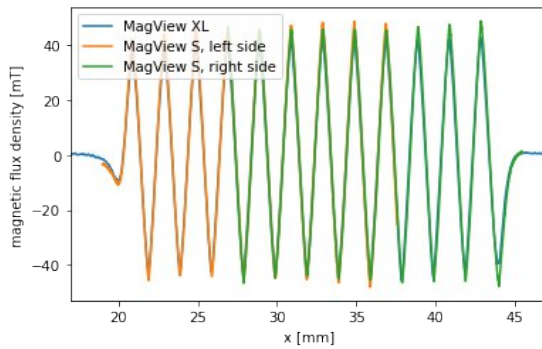
Fig. 6: Flux-density distribution measured by PTB in all pieces of the broken scale 3 with a non-magnetic 500  $\mu\text{m}$  thick spacer with the CMOS-MagView S and the CMOS-MagView XL.

### 3.3 Comparison PTB data

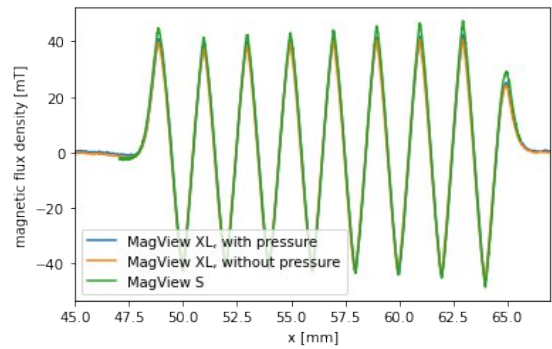
Cross sections of the 2D CMOS\_MagView data were used for the analyses. Cross sections were taken in the direction of the horizontal symmetry axis of the scale. The plotted data show the average over 50 neighboring lines for both CMOS\_MagView systems along the brightened area. The averages for both CMOS-MagView devices is shown below:



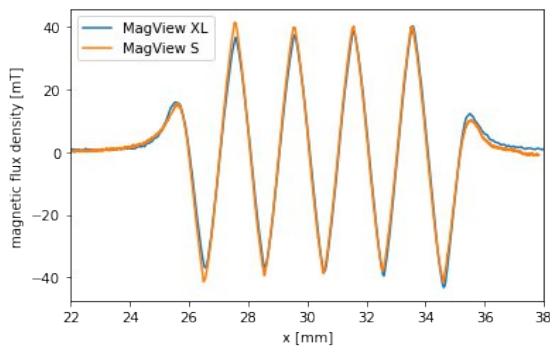
Piece 1



Piece 2



Piece 3



Piece 4

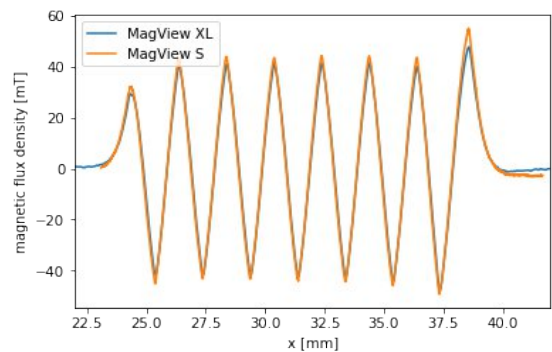


Fig. 7: Flux-density distribution measured by PTB for the broken scale 3 piece No 1 with a non-magnetic 500  $\mu\text{m}$  thick spacer. The area used for averaging is shown in a brighter tone. The resulting averages for all pieces are shown below comparing both CMOS-MagView devices.

The results of both CMOS-MagView devices used at PTB show a good agreement.

## 4 Results TUBITAK

The Sensitec scale 3 was measured at TUBITAK before and after it was broken. TUBITAK used its home-built scanning confocal microscope for the measurements.

### 4.1 Calibration of the TUBITAK confocal microscope

The TUBITAK setup was calibrated by placing the MOIF in a field coil with the bore diameter of 16 mm. The measurements were performed on a spot with the width of 6  $\mu\text{m}$ , thus the field created by the coil can be considered sufficiently homogeneous across the measurement spot. The coil calibration uncertainty is 0.2%. The light intensity was measured as a function of the magnetic field by a photomultiplier tube (PMT) connected to a Lock-in amplifier, which measures the PMT current in nanoamperes. The obtained curves were fitted by a 3rd order polynomial and the fits thus obtained were used to derive the magnetic flux density over the SENSITEC scales.

The light source in the microscope (a halogen lamp) has an adjustable power supply that does not have fixed power settings. That is why calibration had to be performed before each set of measurements (i.e. on each day) as the power supply adjustment might have varied from measurement to measurement. Besides, the calibration has to be repeated if the polarizers in the microscope are re-adjusted. Before starting the calibration, the light source was kept on for 1 hour to thermalise as the gradual temperature change results in a slight variation of its brightness.

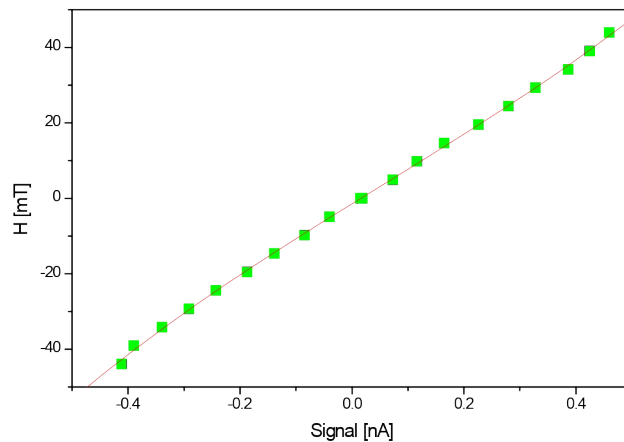


Fig.8: MOIF calibration curve in TUBITAK confocal microscope

An example calibration curve is shown in Figure 8. The polynomial fit results in

$Y = a + bx + cx^2 + dx^3 + ex^4$ , where

$$a = -1.435 \pm 0.226$$

$$b = 91.700 \pm 1.503$$

$$c = -5.6716 \pm 2.386$$

$$d = 36.994 \pm 10.583$$

Here Y stands for the magnetic field in mT and x for the signal measured by the Lock-in amplifier in units of nA.

All calibrations and subsequent measurements were performed at the environment temperature of  $23 \pm 0.5$  °C.

## 4.2 Results TUBITAK

In a first set of measurements, at TUBITAK, flux density measurements were taken of the unbroken scale No3 along the center line of the pole trace using the non-magnetic 500  $\mu\text{m}$  thick spacer. Equidistant data points were taken with a lateral spacing of 50  $\mu\text{m}$ . Three consecutive measurements were taken at the same measurement path. The consecutive measurements show a small offset in the starting point, therefore the datasets were aligned by a correlation analysis. In a second step the point-by-point average of the data was taken over all 3 measurements together with the standard deviation as the uncertainty.

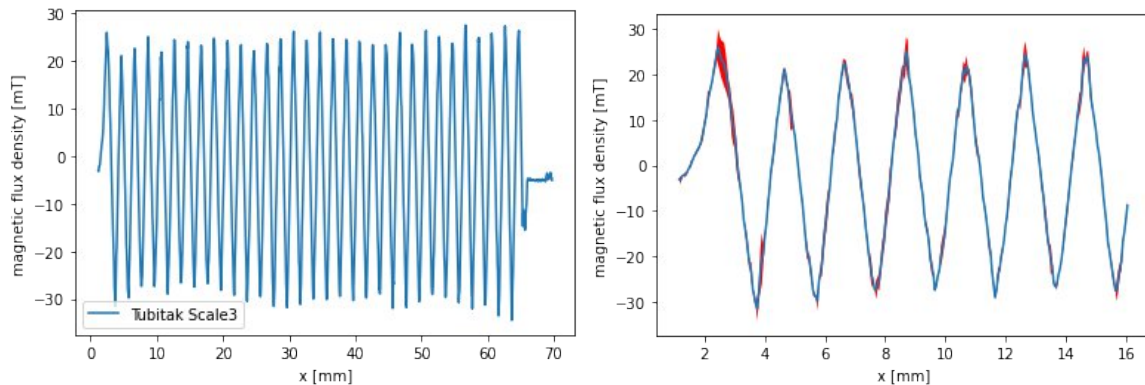


Fig.9: Flux-density distribution of the unbroken scale 3 (left) and close-up of one of the ends of the scale. The red area marks the uncertainty (right) in contact.

The point-by-point average of the data was taken together with the standard deviation as the uncertainty. The three datasets show a very good agreement and thus demonstrate the high reproducibility of the setup.

In a second set of measurements, measurements were performed on the broken scale 3, piece No1 with a 500  $\mu\text{m}$  non-magnetic spacer and with two different objectives. The objectives have an impact on the measured field amplitude, since they determine the imaging spot width of the confocal microscope and thus the area over which the field is averaged. One can see the difference between the peak values in Figure 10 for the measurements done with 5x and 10x objectives. However, there was no difference between the peaks measured with 10x and 20x objectives. This shows that the measurement spot with the 10x objective (the width amounts to 6  $\mu\text{m}$ ) was small enough so that the flux density above the peak cusp is constant across the measurement spot. Thus there was no need to further increase the magnification by using the 20x objective, and all further measurements used for the comparison were done with the 10x objective.

The height of the measurement spot was 200  $\mu\text{m}$ , this determines the area in the vertical direction (perpendicular to the scan) over which averaging was performed (the averaging was performed not digitally as in the case of PTB and Innovent but by measuring an analog signal from a  $6 \times 200$   $\mu\text{m}^2$  rectangular spot).

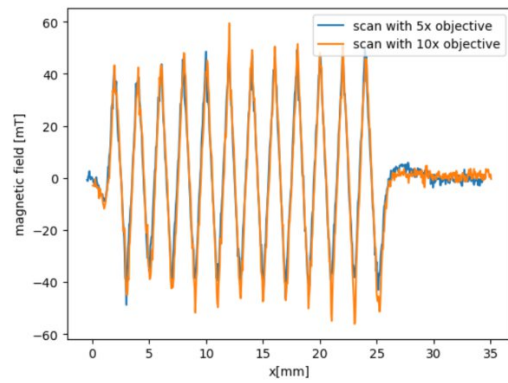


Fig. 10: Flux-density distribution measured by TUBITAK of the broken scale 3 piece No 1 with an non-magnetic 500  $\mu\text{m}$  thick spacer and for objectives with 5x and 10x magnification.

## 5 Results Innovent

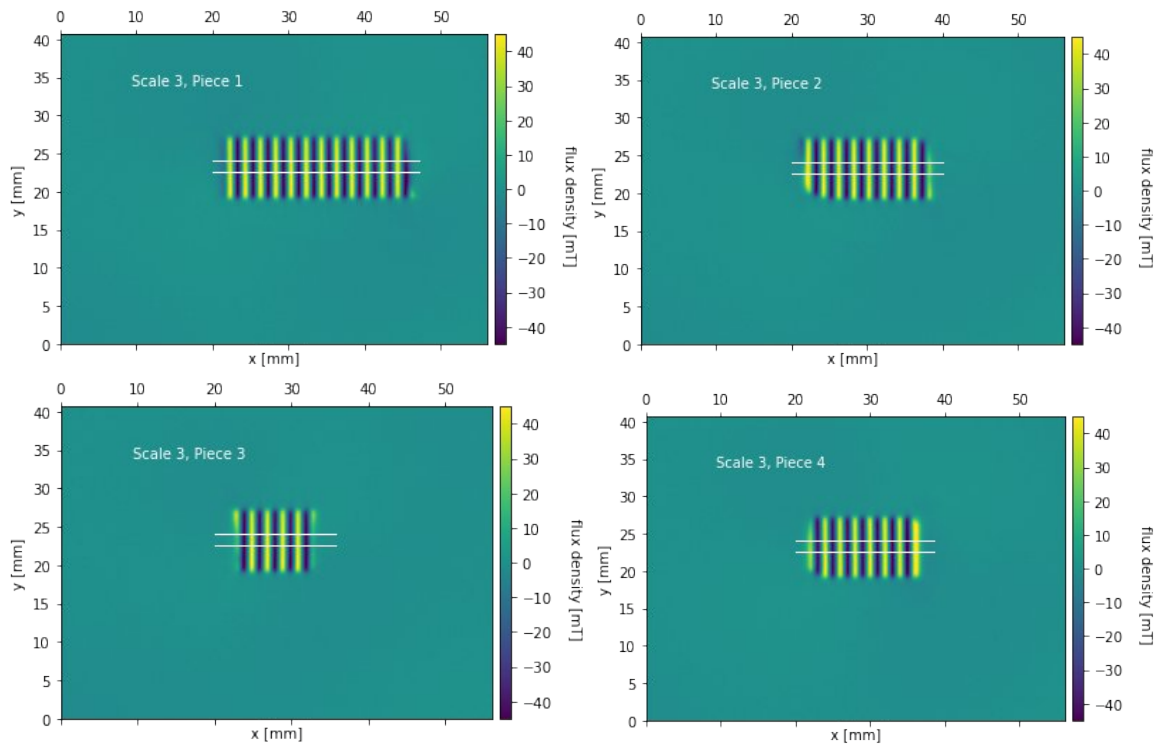
### 5.1 Calibration of the Innovent setup

INNOVENT used a CMOS-MagView XL containing a type C MO sensor (primarily with magnetic in-plane anisotropy) with a pixel resolution of 28.55  $\mu\text{m}$ . The magneto-optical instrument was calibrated for a magnetic field range of  $\pm 125$  mT using a laboratory electromagnet. During calibration, CMOS-MagView was placed between the two pole caps of the electromagnet with the MO sensor surface perpendicular to the dipole field and a Hall probe with a precision of 0.1% was used as a reference. Calibration and measurements were carried out after a warm-up phase of 3 hours of the device at  $RT = 23^\circ\text{C}$ . In addition, the encoder samples were positioned directly at a defined stop to make the magneto-optical measurements reproducible. The magnetic field images were taken using the differential image technique with regard to the homogenization of the whole image and an image averaging of 100x to enhance the signal-to-noise-ratio of every pixel.

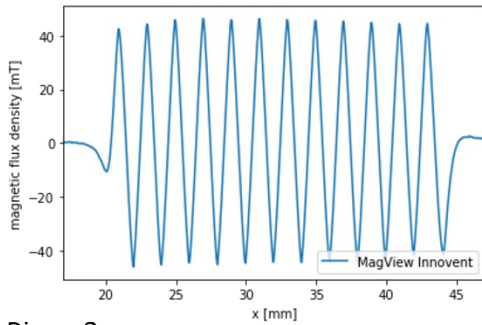
### 5.2 Results Innovent

Measurements were done of all 4 pieces of the broken scale No3 using the same 500  $\mu\text{m}$  thick non-magnetic spacer as used by PTB and TUBITAK.

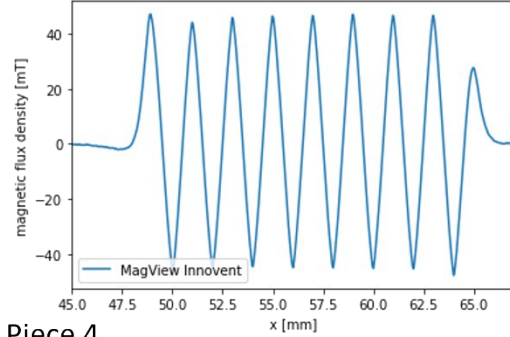
Data CMOS-MagView XL (Innovent):



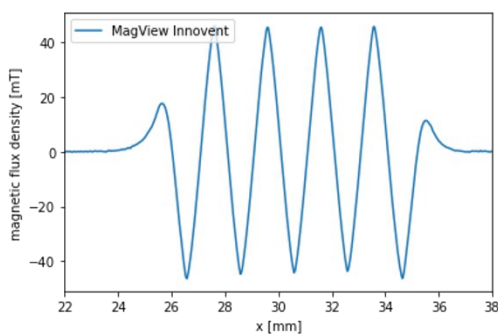
Piece 1



Piece 2



Piece 3



Piece 4

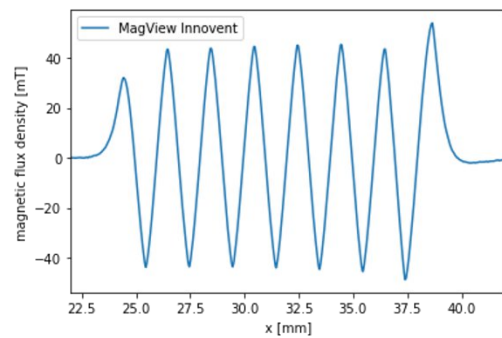


Fig. 11: Flux-density distribution measured by Innovent for all pieces of the broken scale 3 measured with a non-magnetic 500  $\mu\text{m}$  thick spacer. The area between the white lines is used for averaging. The resulting averages for all pieces are shown below for all pieces.

## 6 Comparison between partners

For the comparison the data from all partners measured on scale 3 piece No 1 are used.

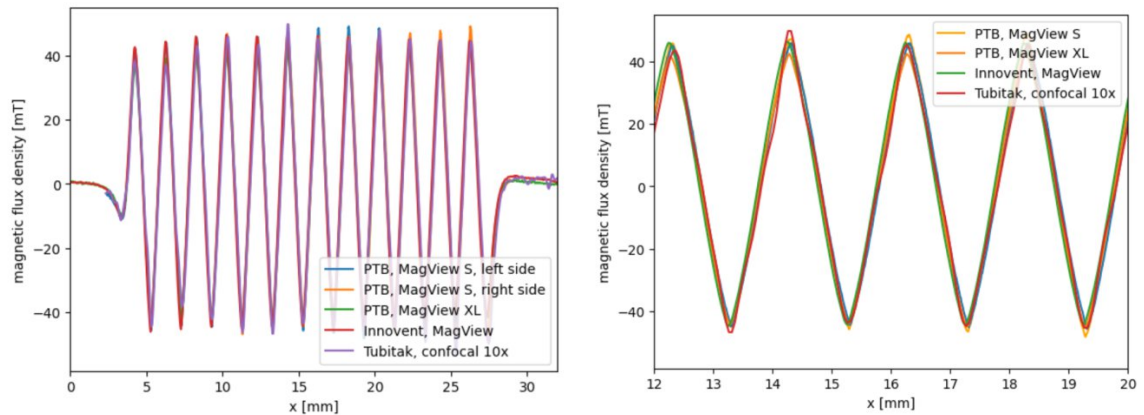


Fig. 12: Flux-density distribution measured on scale 3 piece No 1 measured with a non-magnetic 500  $\mu\text{m}$  thick spacer. The results from all partners and for all used setups are shown. The left image shows the data of the complete piece, the right image shows a zoomed-in view.

The data show a good agreement. For a detailed analysis, the data from PTB and Innovent as well as from PTB and TUBITAK are compared in the following.

### 6.1 PTB and TUBITAK

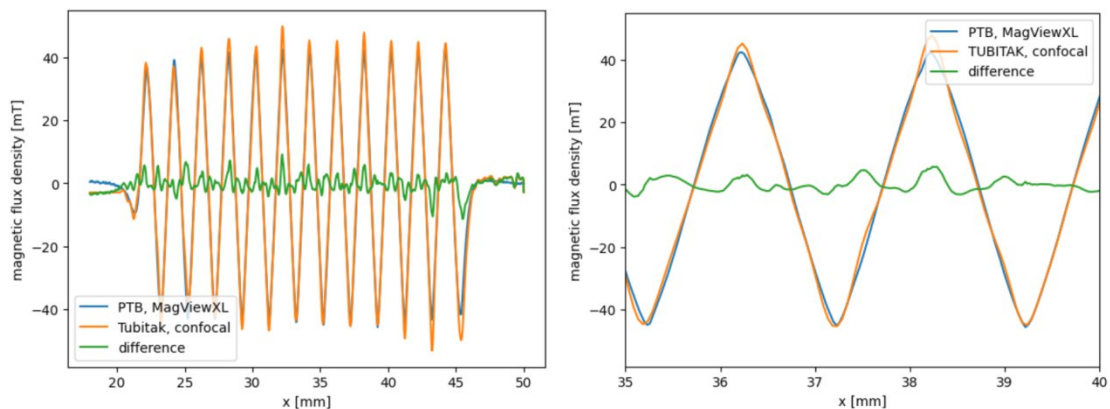


Fig. 13: Flux-density distribution measured on scale 3 piece No 1 with a non-magnetic 500  $\mu\text{m}$  thick spacer. The results from PTB and TUBITAK are shown together with the differences. The left image shows the data of the complete piece, the right image shows a zoomed-in view.

The shape of both profiles is very similar. The average absolute difference  $\overline{\Delta B} = 1.9 \text{ mT}$

### 6.2 PTB and Innovent

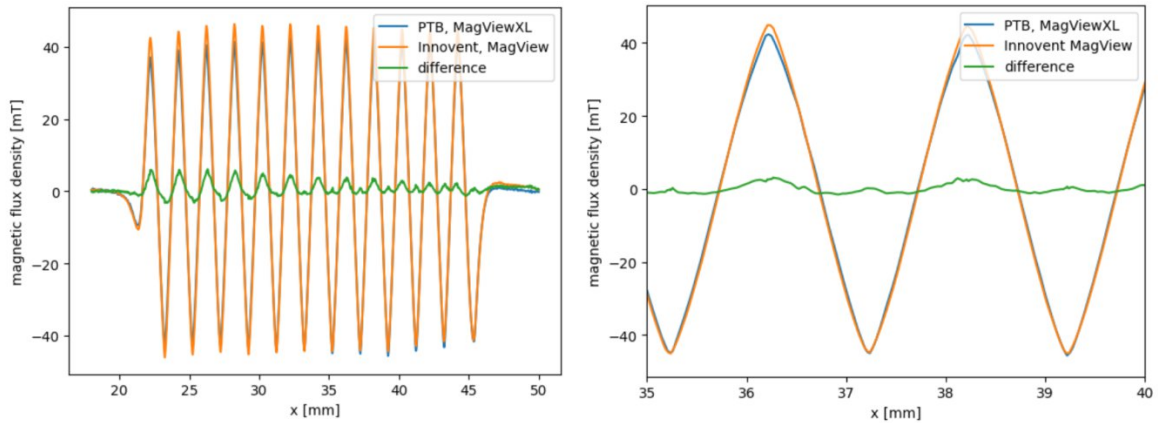


Fig. 14: Flux-density distribution measured on scale 3 piece No 1 with a non-magnetic 500  $\mu\text{m}$  thick spacer. The results from PTB and Innovent are shown together with the differences. The left image shows the data of the complete piece, the right image shows a zoomed-in view.

The shape of both profiles is very similar. As can be seen, the difference between the PTB and Innovent data systematically decreases for higher x-values. We attribute this to a tilt of the scale. The average absolute difference  $\overline{\Delta B} = 1.3 \text{ mT}$

### 6.3 Analysis of pole widths

Pole widths are extracted from images of unbroken scales. To this end the positions of the zero crossings are determined from the data after smoothing by an interpolation.

#### PTB data:

An image of the unbroken scale No1 and the unbroken scale No3 were taken in contact with the sensor using the CMOS-MagView XL:

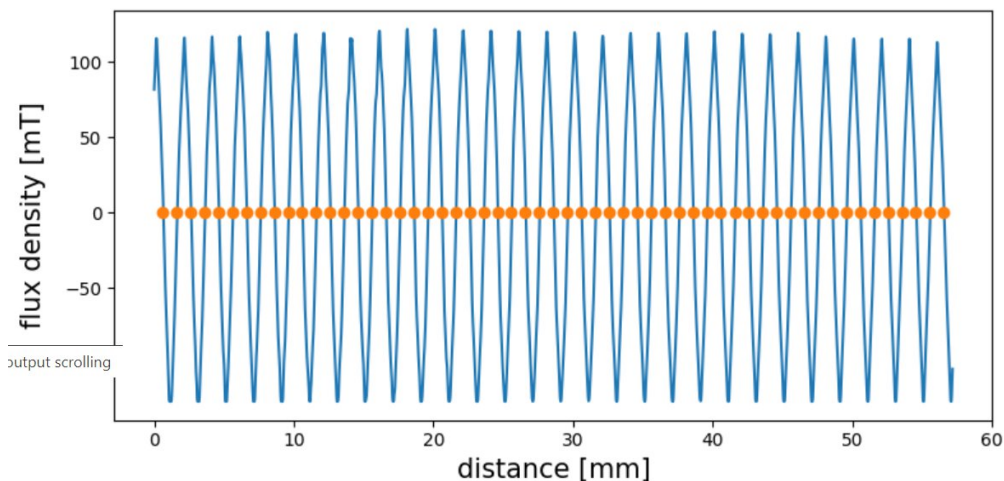


Fig. 15: Flux-density distribution measured by PTB on scale 3 in contact together with the positions of the zero crossings.

The average distance of consecutive zero crossing derived from the scale 1 data

Polewidth<sub>PTB</sub> = (0.9985 +/- 0.0088) mm

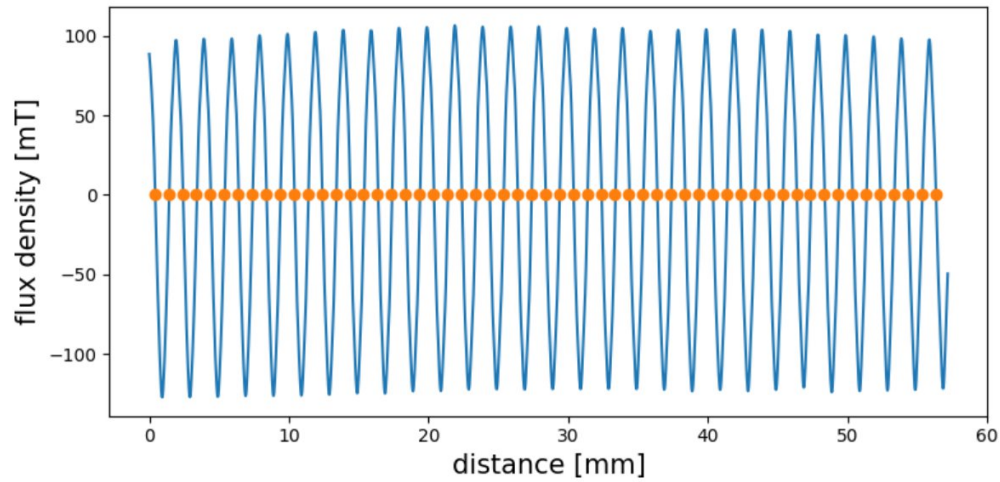


Fig. 16: Flux-density distribution measured by PTB on scale 1 in contact together with the positions of the zero crossings.

The average distance of consecutive zero crossing derived from the scale 1 data

Polewidth<sub>PTB</sub> = (0.9983 +/- 0.0087) mm

**TUBITAK data:**

TUBITAK data were taken from a measurement of the unbroken scale No3 at a distance of 500 μm using the confocal microscope.

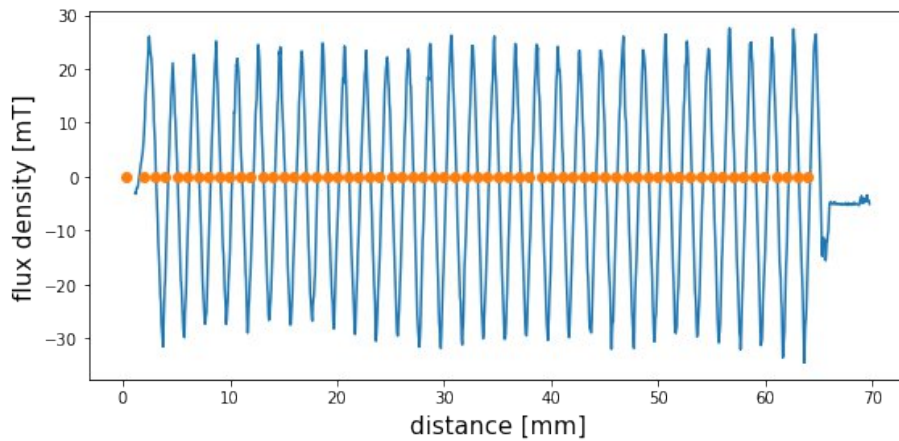


Fig.17: Flux-density distribution measured by TUBITAK on scale 3 in contact together with the positions of the zero crossings.

The average distance of consecutive zero crossing derived from these data is

Polewidth<sub>TUBITAK</sub> = (0.998 +/- 0.0923) mm

**Innovent data:**

An image of the unbroken scale No1 was taken in contact with the sensor using the CMOS\_MagView XL:

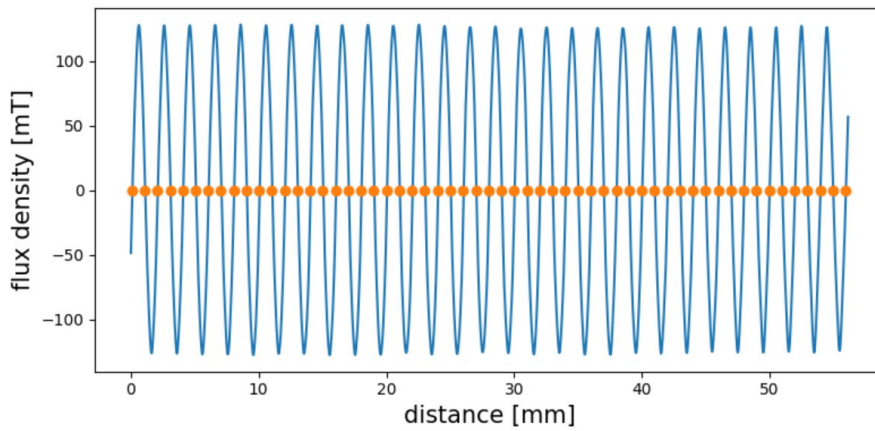


Fig. 18: Flux-density distribution measured by Innovent on scale 1 in contact together with the positions of the zero crossings.

$$\text{Polewidth}_{\text{Innovent}} = (1.00 \pm 0.0049) \text{ mm}$$

### Summary of polewidth data

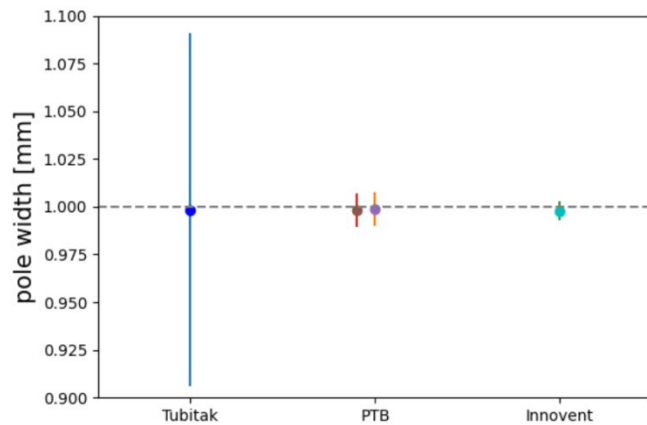


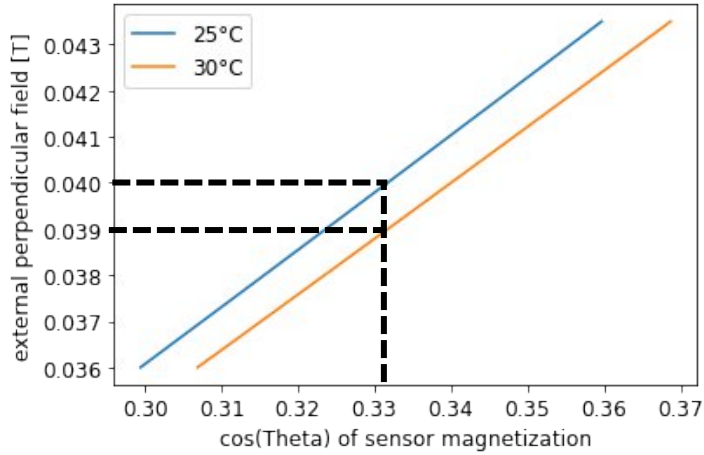
Fig. 19: Pole widths from all measurements together with uncertainties (standard deviation), TUBITAK: scale 3 (confocal microscope), PTB scale 3 (left, CMOS-MagViewXL) and scale 1(right, CMOS-MagViewXL) and Innovent: scale 1 (CMOS-MagView).

All measurements and the results from both scales agree within the error margins. For the CMOS-MagView devices, the error margins are very low, about 1%. The larger error margin for the TUBITAK data can be attributed to the fact, that only data along a single were measured. Furthermore, there is a small field offset visible in the PTB data which systematically shifts the zero crossings.

## 7 Discussion of uncertainties.

### Temperature deviation during calibration

From the known temperature dependent anisotropy terms of the MOIF, the relation between external magnetic field and tilt angle of the sensor magnetization  $\theta$  can be calculated as a function of temperature.



If the MOIF was calibrated at 30°C, but used at 25°C, a measurement at 40 mT would yield a tilt angle of  $\cos(\theta) = 0.332$ , which would be interpreted as 0.39 mT, using the 30° calibration curve. Therefore, the uncertainty contribution of a temperature mismatch is assumed to be 1mT.

### Calibration

Maximum standard deviation of the calibrations at PTB was  $\pm 3$  mT, the standard deviation for subsequent measurements at TUBITAK was  $\pm 3.3$  mT.

### Calibration

The Sensitec scale used in the RRC needs to be aligned for the measurement and ideally is pressed onto the MOIF to guarantee an as small as possible distance to the sensor. However, due to the aspect ratio of the scale, one might expect some tilting of the scale when pressing it onto the MOIF. This might lead to offset fields that are visible in the TUBIAK and some of the PTB measurements.